Earth Planet. Sci. Lett. 640 (2024) 118795

Contents lists available at ScienceDirect

Earth and Planetary Science Letters

journal homepage: www.elsevier.com/locate/epsl

Evolution of tungsten isotope systematics in the Mauna Kea volcano provides new constraints on anomalous $\mu^{182}W$ and high $^{3}He/^{4}He$ in the mantle☆

Lori N Willhite *, Valerie A Finlayson, Richard J Walker

Department of Geology, University of Maryland, College Park, MD 20742, USA

ARTICLE INFO

Keywords:
Mantle plumes
Ocean island basalts
Tungsten isotopes

ABSTRACT

Highly siderophile element abundances and $^{182}W/^{184}W$ and $^{187}Os/^{188}Os$ were determined for a suite of Mauna Kea lavas from the Hawaiian Scientific Drilling Project phase 2 drill core. The new analyses, combined with previous measurements, compose the largest database for $\mu^{182}W$ (the parts-per-million deviation of $^{182}W/^{184}W$ from a terrestrial standard) for a single volcano ($n = 16$). Although most lavas analyzed are characterized by negative $\mu^{182}W$ values, lavas with values similar to the modern bulk silicate Earth are found throughout the entire stratigraphic column. This suggests that components with normal $\mu^{182}W$ are collocated with components that host $\mu^{182}W$ deficits in the plume. Negative $\mu^{182}W$ values are associated with elevated $^{3}He/^{4}He$, as well as elevated Ti and Nb. These correlations may link $\mu^{182}W$ anomalies to ancient deep mantle crystal-liquid fractionation processes. Consistent with previously measured $^{3}He/^{4}He$ (R/R_A) in the drill core, the magnitude of negative $\mu^{182}W$ values was greatest when Mauna Kea was close to the plume axis then generally decreased over the ~400 kyr captured by the stratigraphic section. The component with anomalous $\mu^{182}W$ was either concentrated near the plume axis, or was more effectively sampled by melting near the plume axis where the temperature excess was greatest, suggesting it was less fusible than the dominant plume components. The process leading to the generation of a mantle component with a negative $\mu^{182}W$ anomaly could either be related to some form of core-mantle isotopic equilibration, or early-Earth fractionation within the silicate Earth. At present each possibility remains viable.

1. Introduction

With a half-life of 8.9 Myr (Vockenhuber et al., 2004), the $^{182}Hf \rightarrow ^{182}W$ radiogenic isotope system was extant for only the first ~ 60 Myr of Solar System history. Despite the short lifetime of the system, both ancient and modern terrestrial rocks have been found to exhibit isotopic variability in $^{182}W/^{184}W$ ratios, reflecting variable ingrowth of ^{182}W from ^{182}Hf (Mundl et al., 2017; Willbold et al., 2011). Deficits in $\mu^{182}W$ (the parts-per-million deviation of $^{182}W/^{184}W$ from terrestrial standards believed to be representative of the bulk silicate Earth; BSE) observed in a subset of modern ocean island basalts (OIB) have been interpreted to either reflect some form of core-mantle interaction, or the preservation of isotopic signatures of processes that occurred in the early silicate Earth, such as magma ocean differentiation or grainy late accretion (Archer et al., 2023; Mundl-Petermeier et al., 2020; Peters et al., 2024; Rizo et al., 2019). The observation that, in some OIB systems, increasingly negative $\mu^{182}W$ anomalies correlate with increasing $^{3}He/^{4}He$ provides further evidence for long-term storage of primitive geochemical signals in Earth's interior (Mundl et al., 2017; Mundl-Petermeier et al., 2020; Rizo et al., 2019). The magnitude of $\mu^{182}W$ at a given $^{3}He/^{4}He$ (i.e., the slope in W-He isotopic space) varies by plume locality. In global OIB systems, this has been explained as a result of mixing of at least three components, including ambient mantle, an early-formed mantle reservoir with high $^{3}He/^{4}He$ and normal $\mu^{182}W$, and a core-equilibrated mantle reservoir that has inherited negative $\mu^{182}W$ through isotopic equilibration with the metal core (Mundl-Petermeier et al., 2020).

In the global dataset for recent plume-derived systems, $\mu^{182}W$ does not appear to correlate with lithophile or other siderophile radiogenic isotope compositions (Jackson et al., 2020; Walker et al., 2023), making

☆ Competing Interest Statement: The authors do not declare any competing interests.

* Corresponding author at: Geology Building #237, 8000 Regents Drive, College Park, MD 20742, USA.
E-mail address: LNW@UMD.EDU (L.N. Willhite).

https://doi.org/10.1016/j.epsl.2024.118795
Received 3 March 2024; Received in revised form 10 May 2024; Accepted 19 May 2024

it difficult to link anomalous $\mu^{182}W$ in the mantle to processes such as silicate differentiation or metal-silicate interaction. The magnitude of $\mu^{182}W$ anomalies in plume sources has likely been attenuated by variable mixing among the anomalous component(s), ambient mantle, and W-rich recycled lithosphere (Jackson et al., 2020). Deconvolving the origin and evolution of anomalous $\mu^{182}W$ in the mantle using global OIB, therefore, is challenging due to the complexity of recycled componentry and diverse petrogenesis of volcanic rocks among different plume-derived systems.

Here, we focus on the $\mu^{182}W$ and $^3He/^4He$ systematics of a single volcano over time, the Mauna Kea volcano, as sampled by the Hawaiian Scientific Drilling Project phase 2 core (HSDP-2). Detailed study of a single volcano limits the complexity of mantle source componentry, and permits addressing questions that include: (1) Are $\mu^{182}W$ and $^3He/^4He$ systematics consistent with two-component mixing within a single volcano? (2) Do other petrologic and/or geochemical parameters correlate with $\mu^{182}W$ or predict W-He behavior? (3) Do stratigraphic variations in $\mu^{182}W$ and $^3He/^4He$ inform plume structure and dynamics?

The HSDP-2 yielded a ~3500 meter long core representing a ~ 680 kyr record of volcanism (Sharp and Renne, 2005). The majority of the stratigraphic section comprises lavas from the Mauna Kea volcano, although ~250 m of Mauna Loa lavas were also sampled in the upper section of the drill core. We report new $\mu^{182}W$ data for twelve Mauna Kea lavas. These same lava flows have been previously characterized for, and represent a range of, $^3He/^4He$ and petrologic type (Kurz et al., 2004; Rhodes and Vollinger, 2004). The new $\mu^{182}W$ values are combined with four previous $\mu^{182}W$ analyses from HSDP-2 (Mundl et al., 2017; Mundl-Petermeier et al., 2020). These data allow investigation of the W-He systematics of the volcano over a well-defined period of time (Table 1). Although the focus of this study is Mauna Kea, we also report three new $\mu^{182}W$ data from the Mauna Loa section at the top of the drill core for comparison with Mauna Kea. Mauna Kea and Mauna Loa volcanoes represent the archetypal volcanoes of the respective geographic and geochemical "Kea" and "Loa" trends that have been identified in Hawaii (Abouchami et al., 2005). The two trends have been interpreted to reflect sampling of distinct deep mantle sources (Weis et al., 2011) and have implications for the structure and dynamics of the Hawaiian mantle plume. Therefore, whether there are distinct $\mu^{182}W$ and $^3He/^4He$ systematics of the two trends warrants investigation.

2. Methods

2.1. Tungsten isotopic analyses

Tungsten isotopic compositions were analyzed via negative-ion thermal ionization mass spectrometry (N-TIMS) on a *Thermo Scientific Triton*™ multicollector thermal ionization mass spectrometer in the Isotope Geochemistry Laboratory at the University of Maryland, College Park. Details on sample preparation, including chemical separation methods for isotopic analysis, are provided in the supplementary materials. Laboratory total procedural blanks for W chemistry averaged 380 pg and were always well below 1% of the total W. Following chemical separation, approximately 1000 ng of W was loaded onto Re filaments in 1 μL of 0.5 M HCl + 0.5 M HF and dried down. After letting the loaded W sit on the Re filament overnight, 1 μL of La (9 ng/μL) and Gd (3 ng/μL) activator was added to improve ionization of W. Mass spectrometric measurements followed the Faraday cup and amplifier configuration and per-integration oxide correction from (Archer et al., 2017). Typical beam intensities were ~1 V on mass $^{184}WO_3$ using 10^{11} Ω resistor amplifiers and analysis time was 12 h and 15 min per sample, including 45 min of baseline measurements.

Isotopic ratios were corrected for mass fractionation assuming an exponential law and normalizing to $^{186}WO_3/^{184}WO_3$ of 1.9859 (additional normalization schemes are presented in Supplementary Tables S1 and S2 for standards and samples, respectively). $^{181}TaO_3$ was monitored for $^{180}TaO_3$ isobaric interference on $^{180}WO_3$. Tungsten oxide isotopologues including ^{18}O (e.g., $^{186}W^{16}O_2^{18}O$) were measured using 10^{12} Ω resistor amplifiers to improve signal to noise of low abundance oxides and correct for O isotope variability (Archer et al., 2017). The *Alfa Aesar* W standard (Lot No.: 211576 G) was analyzed repeatedly throughout the analytical sessions ($n = 21$) with an average $^{182}W/^{184}W$ (normalized to $^{186}W/^{183}W = 1.9859$) of 0.864861 and an external reproducibility of 2.9 ppm (2SD) and 0.6 ppm (2SE; Supplementary Table S1).

2.2. Determination of W concentration

Tungsten concentrations were determined using the isotope dilution method with ~100 mg fractions of the same sample powders generated for W isotopic analysis. Following addition of a ^{182}W spike, dissolution, and chemical separation (described in the supplementary material), the

Table 1
New (bold) and previously published $\mu^{182}W$, $^{187}Os/^{188}Os$, and W concentration data, as well as previously published $^3He/^4He$ and MgO wt.% for lavas from the Hawaiian Scientific Drilling Project 2.

Sample	Volcano	MgO wt.%	Depth (mbsl)	Model age (ka)	$\mu^{182}W$ (6/3)	2SE	W ppb	$^3He/^4He$ (R/R_A)	(1σ)	$^{187}Os/^{188}Os$
SR0008–4.2	ML	7.64	−9.5		**1.9**	**2.4**	**109**	8.0	0.1	**0.1360**
SR0113–6.1	ML	18.72	−222.5		**−3.7**	**3.7**	**45**	14.6	0.2	**0.1332**
SR0117–3.8	ML	19.42	−234.6		**−6.5**	**4.0**	**130**	17.6	0.2	**0.1335**
SR0167–5.7	MK	8.94	−378.4	312.8	**−2.6**	**2.2**	**96**	7.3	0.6	**0.1293**
SR0267–6.3	MK	23.16	−615.8	353.7	**−2.9**	**3.0**	**131**	8.2	0.3	**0.1282**
SR0372–3.2	MK	8.17	−871.2	381.8	**−4.3**	**3.6**	**119**	11.5	0.1	**0.1295**
SR0455–6.8	MK	26.01	−1098.2	406.8	**−4.0**	**3.1**	**54**	12.3	0.1	**0.1291**
SR0548–8.0	MK	19.5	−1404.1	440.5	**−8.6**	**3.4**	**96**	10.3	0.04	**0.1289**
SR0683–5.75	MK	19.55	−1763.3	480.0	−1.8	4.7	**70**	10.7	1.5	**0.1297**
SR0750–12.45	MK	17.23	−2032.8	512.9	−11.5	5.2	114	23.2	0.1	**0.1296**
SR0756–14.3	MK	18.91	−2098.6	516.8	**−6.3**	**3.2**	**103**	17.4	0.1	0.1295
SR0762–4.6	MK	17.93	−2123.8	519.6	−8.7	3.5	**64**	19.8	0.8	**0.1301**
SR0860–6.5	MK	7.77	−2615	573.7	**−5.8**	**3.5**	**160**	16.5	0.2	**0.1293**
SR0891–15.10	MK	22.04	−2730.4	586.3	−10	3.7	90	14.0	0.1	0.1299
SR0913–2.3	MK	12.47	−2825.8	596.8	**−3.2**	**2.3**	**98**	14.9	0.1	**0.1303**
SR0940–7.7	MK	13.59	−2967.8	612.5	**−16.6**	**3.8**	**110**	21.0	0.1	**0.1291**
SR0954–7.4	MK	18.03	−3009.2	617.0	**−12.0**	**3.6**	**99**	13.9	0.1	**0.1276**
SR0956–9.3	MK	7.01	−3019	618.1	**−12.1**	**3.7**	**156**	12.8	0.2	**0.1300**
SR0967–2.8	MK	15.39	−3068	623.6	**−3.8**	**3.3**	**114**	11.9	0.1	**0.1295**

$\mu^{182}W$ is the deviation of $^{182}W/^{184}W$ of a sample from that of the average of repeated measurements of an Alfa Aesar tungsten standard (2SD = 2.9; $n = 21$). New data are presented in bold. The 2SE represents the internal standard error of a single analysis. All $\mu^{182}W$ values are normalized to $^{186}W/^{183}W$; other normalizations are given in Supplementary Table S2. ML = Mauna Loa. MK = Mauna Kea. MgO wt.% is from Rhodes and Vollinger (2004). Depth, age, and $^3He/^4He$ are from Kurz et al. (2004). Previous $\mu^{182}W$ and W concentration data are from Mundl et al. (2017) and Mundl-Petermeier et al. (2020). Previous $^{187}Os/^{188}Os$ data are from Ireland et al. (2009b).

W fraction was measured by multi-collector inductively-coupled-plasma mass spectrometry (MC-ICP-MS) using a *Thermo Scientific Neptune Plus* instrument in the Plasma Laboratory at the University of Maryland, College Park. The total procedural blanks for W isotope dilution measurements ranged from 14 to 50 pg, which is less than 0.5% of the W mass from the sample.

2.3. Highly-siderophile element concentrations and Os isotopic composition

Separation of highly siderophile elements (HSE) utilized Carius tube digestion followed by solvent extraction and microdistillation to purify Os, and anion exchange column chemistry for *Re*, Ru, Pd, Ir, and Pt (see supplementary material). The Os fraction was analyzed by N-TIMS for Os concentration and $^{187}Os/^{188}Os$ using the *Thermo Scientific Triton* in the Isotope Geochemistry Laboratory at the University of Maryland, College Park. Analytical precision (internal 2SE) for all samples was less than 0.15 %. Total procedural blanks for Os averaged 1.9 pg. Following chemical separation, Re, Ru, Pt, Ir, and Pd were analyzed using the *Thermo Scientific Neptune Plus* MC-ICP-MS instrument in the Plasma Laboratory at the University of Maryland, College Park. Average total procedural blanks for Re, Ru, Pt, Ir, and Pd were 2.4, 34, 13, 1.1, and 18 pg.

3. Results

3.1. Tungsten concentration and isotopic composition of HSDP-2 lavas

Tungsten concentrations of Mauna Kea lavas from HSDP-2 range from 45 to 160 ppb. The W/Th of the samples range from 0.08 to 0.24, all of which are within the range cited for the canonical value (e.g., 0.19 ± 0.15) for the BSE estimated from global mantle-derived lavas (Arevalo and McDonough, 2008). Tungsten concentration varies as an approximately sigmoidal function of MgO wt.% (Fig. 1). The $\mu^{182}W$ values of Mauna Kea lavas measured in this study range from −1.8 to −16.6, while Mauna Loa lavas analyzed in this study have $\mu^{182}W$ that ranges from +1.9 to −6.5. The typical analytical uncertainty for $\mu^{182}W$ of the samples was 3.3 ppm (internal 2SE). There is no correlation evident between $\mu^{182}W$ and W concentration in this dataset (Supplementary Figure S1). Given the 2.9 ppm (2SD) and 0.6 ppm (2SE) reproducibility of the *Alfa Aesar* W standard, eight out of the nineteen HSDP-2 samples have $\mu^{182}W$ values that are resolvable from the two standard deviation of the terrestrial standard and thirteen are resolvable from the two standard error of the standard (Table 1, Fig. 2). As a measure of data quality, the $\mu^{183}W$ (i.e., $^{183}W/^{184}W$ normalized to $^{186}W/^{184}W$) of the samples was monitored (Supplementary Table S2). The average $\mu^{183}W$ of all HSDP-2 samples was +1.5 ± 4.6 (2SD) and there is no correlation between $\mu^{182}W$ and $\mu^{183}W$ regardless of which isotopic ratio $\mu^{182}W$ is normalized to (Supplementary Figure S2). Previously observed correlations between $\mu^{182}W$ and $\mu^{183}W$, as well as between $\mu^{182}W$ and mass of W processed through chemistry, have been attributed to an analytical origin (Archer et al., 2023); neither correlation is observed in the dataset presented here.

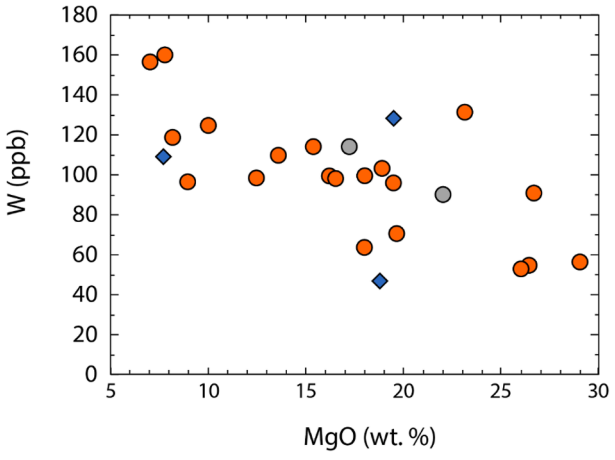

Fig. 1. Tungsten concentration (ppb) versus MgO (wt.%) of HSDP-2 lavas. Orange circles represent new W concentration measurements for Mauna Kea. Grey circles represent W concentrations of Mauna Kea from previous studies (Mundl et al., 2017). Blue diamonds represent new Mauna Loa data. Uncertainties for MgO and W concentrations are smaller than the symbols. For all samples, MgO wt.% is from Rhodes and Vollinger (2004).

Resolvable $\mu^{182}W$ deficits are more prevalent in the lower portion of the 3000-meter-long stratigraphic column, where the greatest magnitude anomalies and the greatest variation of $\mu^{182}W$ values are also observed. Mauna Kea HSDP-2 lavas exhibit a correlation between $\mu^{182}W$ and $^{3}He/^{4}He$ (i.e., Pearson's correlation coefficient $R^2 = 0.4$; p-value = 0.009, where a significant p-value is <0.05; Fig. 4). Normal W isotopic compositions (i.e., $\mu^{182}W = 0 \pm 3.3$) appear throughout the entire stratigraphic section. There is a rebound to larger magnitude $\mu^{182}W$ and $^{3}He/^{4}He$ observed at the transition from Mauna Kea to Mauna Loa volcanics in the HSDP-2 drill core.

3.2. Highly siderophile element concentrations and Os isotopic compositions

Highly siderophile element abundances and $^{187}Os/^{188}Os$ are summarized in Supplementary Table S3. Osmium, Ir, and Ru are positively correlated with MgO wt.% (Supplementary Figure S3). Rhenium concentrations are inversely proportional to MgO wt.% (Supplementary Figure S3). Platinum and Pd abundances are not correlated with MgO content, and Pt abundances exhibit the least variance among HSDP-2 lavas (Supplementary Figure S3). There is no correlation between Pt abundance (or any HSE abundance) and $\mu^{182}W$ in HSDP-2 lavas (Supplementary Figure S4).

The new Mauna Kea data are characterized by $^{187}Os/^{188}Os$ that range from 0.1276 to 0.1306 (Table 1). Consistent with previous studies, the three Mauna Loa samples examined in this study are more radiogenic than the Mauna Kea lavas, with $^{187}Os/^{188}Os$ ranging from 0.1332 to 0.1396 (Brandon et al., 1999; Bryce et al., 2005; Ireland et al., 2009b). There is no correlation between $^{187}Os/^{188}Os$ and Pt concentration (Supplementary Figure S5).

4. Discussion

4.1. Highly siderophile element abundance and Os isotopic characteristics of HSDP-2 lavas

Mauna Kea samples from HSDP-2 are depleted in Os, Ru, Ir, Pt, and Pd relative to the BSE (Fig. 3). Rhenium abundances are typically similar to or enriched compared to BSE. Mauna Loa samples have similar absolute and relative HSE abundances to Mauna Kea in HSDP-2 (Fig. 3). Platinum does not vary with whole rock MgO, as the incompatible (Re) and compatible (Os, Ir, Ru) HSE vary negatively and positively with MgO wt.%, respectively (Supplementary Figure S3). During igneous differentiation, Pt is not strongly compatible in olivine, chromite, or sulfide (Pitcher et al., 2009). Therefore, Pt is not highly fractionated from the source composition. Since there is no covariation of Pt abundance with $\mu^{182}W$, it is concluded that the anomalous $\mu^{182}W$ component is not associated with strongly elevated HSE abundances in Mauna Kea's mantle source.

Mauna Kea lavas have relatively un-radiogenic $^{187}Os/^{188}Os$ compared to other Hawaiian volcanic centers (Ireland et al., 2009b; Lassiter and Hauri, 1998). This may indicate a lesser proportion of recycled oceanic crust and sediments contributing to melts generated in the Mauna Kea source region compared to the sources of other Hawaiian volcanic centers (Lassiter and Hauri, 1998). In HSDP-2 Mauna Kea lavas,

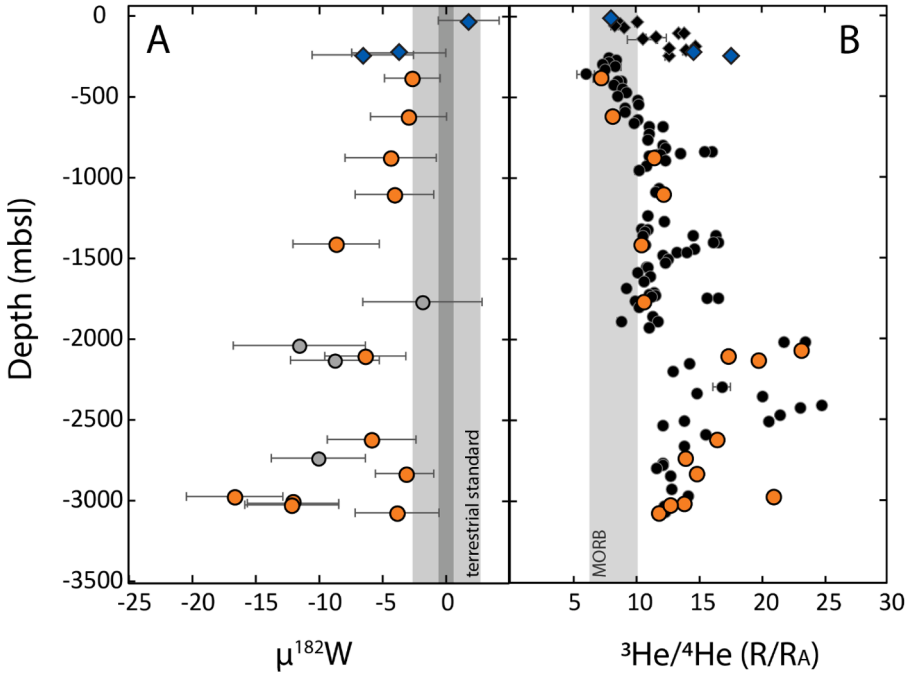

Fig. 2. Tungsten and helium isotopic compositions as a function of stratigraphic depth (meters below sea level). (A) The orange circles are new $\mu^{182}W$ measurements for Mauna Kea volcanics from HSDP-2. Blue diamonds are new $\mu^{182}W$ measurements for Mauna Loa volcanics from HSDP-2. Grey symbols represent previously published $\mu^{182}W$ data (Mundl et al., 2017; Mundl-Petermeier et al., 2020). Vertical grey bands reflect the 2SD (light grey) and 2SE (dark grey) external reproducibility of the *Alfa Aesar* W standard. (B) Orange circles represent Mauna Kea samples that have been characterized for both $^3He/^4He$ and $\mu^{182}W$. Blue diamond symbols represent Mauna Loa samples that have been characterized for both $^3He/^4He$ and $\mu^{182}W$. Black circles and diamonds represent $^3He/^4He$ measurements that do not have paired $\mu^{182}W$ analyses. All He data are from Kurz et al. (2004). The vertical grey band reflects the typical range of $^3He/^4He$ (8 ± 2 R/R_A) observed in global MORB distal from mantle plumes (Graham, 2002).

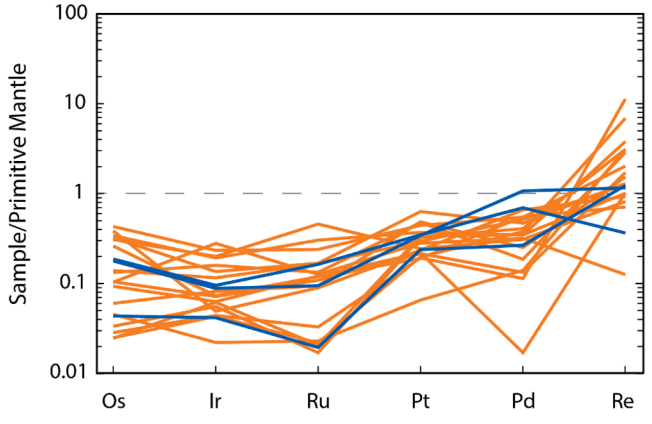

Fig. 3. Primitive mantle (Becker et al., 2006) normalized highly siderophile element abundances of Mauna Kea (orange) and Mauna Loa (blue) samples from HSDP-2.

there is no correlation between Pt abundance and $^{187}Os/^{188}Os$ indicating that the HSE abundance of the mantle source is not related to variation in $^{187}Os/^{188}Os$ observed in the lavas. Additionally, there is no evidence for a relationship between $^{187}Os/^{188}Os$ and $\mu^{182}W$ in Mauna Kea to suggest coupling of $\mu^{182}W$ with siderophile, radiogenic isotope systematics (Supplementary Figure S6).

4.2. Tungsten composition and isotope systematics of the Mauna Kea volcano

Ireland et al. (2009a) estimated that the W concentration of the Mauna Kea source was 8 ± 7 ppb W. This concentration overlaps with estimates of both the BSE, 13 ± 10 ppb W, and the depleted MORB mantle (DMM), 3.0 ± 2.3 ppb W (Arevalo and McDonough, 2008). The canonical W/Th ratios of Mauna Kea lavas reported here support the contention that the Mauna Kea source is not strongly enriched in W relative to other OIB or the DMM. Nevertheless, the estimated W abundance for the Mauna Kea mantle source is permissive of, but does not require, entrained recycled material, a less geochemically depleted mantle source, or core material. Additionally, there is no relationship between W concentration and isotopic composition within the HSDP-2 Mauna Kea lavas to indicate that anomalous $\mu^{182}W$ is hosted by a W-rich component or phase in the plume, or that W-rich recycled components have attenuated negative $\mu^{182}W$ values to produce the normal, BSE-like $\mu^{182}W$ of a subset of the HSDP-2 lavas (Supplementary Figure S1).

The new HSDP-2 $\mu^{182}W$ data, combined with corresponding published $^3He/^4He$ data from the same lava flows, are broadly consistent with the previously reported Hawaiian W-He trend defined by lavas from Mauna Kea, Mauna Loa, Kohala, Kīlauea, and Kamaʻehuakanaloa volcanic centers (Fig. 4). Variation in the Hawaiian suite cannot be accounted for by a simple two-component mixing model. Thus, as with the global OIB database, a minimum of three component mixing may be required to explain the variance among Hawaiian volcanic centers, although some shallow plume processes may decouple $\mu^{182}W$ from $^3He/^4He$, leading to data that diverge from two-component mixing models (see Supplementary Material S.4).

For Mauna Kea lavas, the scatter in $\mu^{182}W$ and $^3He/^4He$ space is less than for the entire Hawaiian suite. This may, in part, reflect the fact that Mauna Kea lavas do not capture the extreme W and He isotopic compositions observed in other volcanic centers in Hawaii, particularly Kamaʻehuakanaloa. In Mauna Kea, the correlation between $\mu^{182}W$ and $^3He/^4He$ is statistically robust ($R^2 = 0.4$; p-value $= 0.009$).

In order to assess whether simple two-component mixing can account for the W-He variations present in the Mauna Kea suite, multiple mixing models were considered. It is found that certain two-component

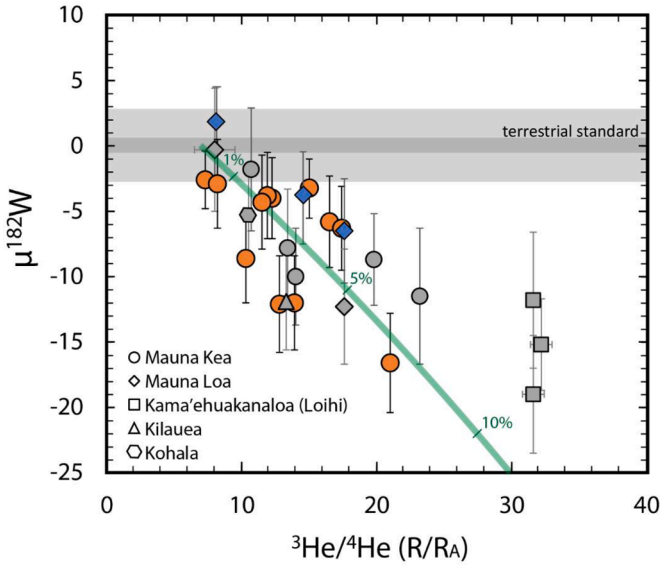

Fig. 4. Tungsten isotopic composition versus $^{3}He/^{4}He$ (Kurz et al., 2004) for all Hawaiian lavas characterized thus far. The orange circles are new $\mu^{182}W$ measurements for Mauna Kea volcanics from HSDP-2. Blue diamonds are new $\mu^{182}W$ measurements for Mauna Loa volcanics from HSDP-2. Grey symbols represent previously published data (Mundl et al., 2017; Mundl-Petermeier et al., 2020). The green band is a mixing curve between ambient and an anomalous component (details in the text). Tick marks show the compositions with 1, 5, and 10% contributions of the low $\mu^{182}W$, high $^{3}He/^{4}He$ component.

mixing models can account for nearly all Mauna Kea samples within the analytical uncertainties (Fig. 4; Supplementary Material S.4). For example, in the solid-solid mixing model presented in Fig. 4, the isotopic composition of the ambient mantle is defined by a He isotopic composition of 7 R/R_A, within the range of typical MORB (Graham, 2002), a ^{4}He concentration estimated for primitive mantle of approximately 1×10^{-5} cm^3 STP/g (Gonnermann and Mukhopadhyay, 2007), and $\mu^{182}W$ of 0. The isotopic composition of the anomalous endmember is defined by a possible core isotopic composition of $\mu^{182}W = -220$ (Kleine and Walker, 2017) and $^{3}He/^{4}He$ of 120 R/R_A (Mahaffy et al., 1998). The W concentration for both endmembers is assumed to be the same as the BSE, ~13 ppb (Arevalo and McDonough, 2008) and the He concentration of the anomalous component is defined as having a ^{4}He concentration of 2×10^{-5} cm^3 STP/g (Ballentine et al., 2002; Gonnermann and Mukhopadhyay, 2007; Mahaffy et al., 1998). The W-He composition of the anomalous component may be characteristic of mantle source at the core-mantle boundary if there was isotopic equilibration between the core and the mantle component (e.g., Ferrick and Korenaga, 2023), and is considered further below. By contrast, a solid-solid mixing model in which the ambient mantle endmember is defined by $\mu^{182}W$ of 0, but a substantially lower W concentration of 3 ppb, representative of the DMM (Arevalo and McDonough, 2008), fails to capture the majority of the Mauna Kea data (Supplementary Figure S7A). Further details and additional mixing scenarios (Supplementary Figures S7A-C) are described in Supplementary Material S.4 and parameters are reported in Supplementary Table S4.

4.3. Tungsten-He correlations with other geochemical parameters?

Although mixing involving hypothetical mantle that isotopically equilibrated with the core can satisfy model requirements for the anomalous component of the Mauna Kea source, the true origin of the anomalous $\mu^{182}W$ and elevated $^{3}He/^{4}He$ remains unknown. The $\mu^{182}W$ deficits and the correlation between $\mu^{182}W$ and $^{3}He/^{4}He$ in OIB have previously been interpreted to have resulted from early silicate differentiation, or uneven mixing of late accreted materials into the mantle, termed *grainy late accretion*, in addition to isotopic equilibration with the metallic core (Archer et al., 2023; Ferrick and Korenaga, 2023; Mundl-Petermeier et al., 2020; Rizo et al., 2019). Identification of correlations between $\mu^{182}W$-$^{3}He/^{4}He$ and other geochemical parameters could narrow the possible options for the generation of the anomalies.

Tungsten isotopic compositions in Mauna Kea do not correlate with $^{87}Sr/^{86}Sr$, $^{176}Hf/^{177}Hf$, or $^{187}Os/^{188}Os$ (Supplementary Figure S8). Thus, the mantle componentry recorded by these isotopic systems does not appear related to the expression of $\mu^{182}W$ in the erupted basalts. Moreover, although data are limited, Hawaiian lavas do not appear to exhibit a correlation between $\mu^{182}W$ and the $^{146}Sm \rightarrow ^{142}Nd$ ($t_{1/2}$ = 103 Myr) system, that could provide corroborative evidence for early silicate differentiation as the origin of $\mu^{182}W$ variation (Horan et al., 2018). Given the absence of significant correlations between $\mu^{182}W$ and other long- and short-lived isotopic systems in Hawaiian lavas characterized thus far, if silicate differentiation while ^{182}Hf was extant produced $\mu^{182}W$ variability in the Hawaiian plume source, supporting isotopic evidence for the ancient Hf/W fractionation event may have since been overprinted by subsequent differentiation or mixing events.

Certain types of core-mantle interactions or the effects of grainy late accretion might be expected to lead to correlations between $\mu^{182}W$ and HSE source abundances, given the high HSE abundances in the metallic core and bulk chondrites (Peters et al., 2023; Puchtel et al., 2016; Touboul et al., 2012; Walker et al., 2023). Correlation between $\mu^{182}W$ and Ru/Ir has been previously observed within a group of Hawaiian lavas from Mauna Kea, Mauna Loa, Kama'ehuakanaloa, Kīlauea, and Kohala, and was inferred to reflect low-pressure, metal-silicate equilibration that occurred early in Earth's history (Peters et al., 2023). Neither $\mu^{182}W$ nor $^{3}He/^{4}He$, however, correlate with Ru/Ir in the Mauna Kea HSDP-2 dataset (Supplementary Figure S9). Direct metal transfer from the liquid outer core into the silicate mantle would significantly elevate the abundances of siderophile elements in the affected mantle. For example, entrainment of core metal with 470 ppb W (McDonough, 2003) and $\mu^{182}W = -220$ (Kleine and Walker, 2017), into the lower mantle would require ~0.25 wt.% of core metal to generate a $\mu^{182}W$ of −18, which is within uncertainty of the largest $\mu^{182}W$ deficit observed in HSDP-2 (Supplementary Table S4). However, the addition of 0.25 % of outer core metal with a Pt concentration of 5700 ppb (McDonough, 2003) would elevate the Pt abundance of the mantle source to ~22 ppb, which is unlikely to produce the range of Pt abundances observed in HSDP-2 lavas (0.5 to 4.8 ppb Pt).

As discussed above, core-mantle interaction may also involve a mechanism that does not directly transfer siderophile elements from the core to the silicate mantle, as would occur with metal infiltration. Previously proposed mechanisms include preferential transfer of W from the core relative to HSE, via oxide exsolution (Rizo et al., 2019), grain boundary diffusion of W from the core (Yoshino et al., 2020), or isotopic equilibration of W between the mantle and core without net mass transfer of W (Ferrick and Korenaga, 2023; Mundl-Petermeier et al., 2020). These mechanisms could occur at any time throughout Earth's history. A core-equilibrated mantle reservoir would not necessarily inherit elevated abundances of W and HSE or coupled ^{182}W-^{142}Nd signatures (Mundl-Petermeier et al., 2020).

Conversely, the presence of relatively unmodified, excess late accreted materials in the anomalous mantle source component would generate negative $\mu^{182}W$ and elevated abundances of siderophile elements in the mantle source. For example, an isolated, BSE-like mantle reservoir with 0.8 wt.% excess chondritic material with 1220 ppb Pt (Horan et al., 2003), 150 ppb W, and $\mu^{182W} = -190$ (Kleine et al., 2004) would have a $\mu^{182}W$ of −16, similar to the maximum observed $\mu^{182}W$ deficit in Mauna Kea (Supplementary Table S4). The solid mantle mixture of BSE with an excess chondritic-like component would have 17 ppb Pt. Given that Pt is not substantially fractionated from the source composition, a mantle source with 17 ppb Pt is higher than may be presumed, given the Pt abundances observed in Mauna Kea melts, and estimated parental melt of 2.3 ± 0.2 ppb Pt (Ireland et al., 2009b).

Isolation and preservation of an excess late accreted material in the deep mantle, thus, would likely elevate the HSE abundances to the extent that it would be detected.

In contrast to long- and short-lived isotope systems, as well as most lithophile and siderophile element abundances, $\mu^{182}W$ in the drill core lavas is characterized by robust correlations with certain high field strength elements (HFSE), consistent with the prior observation of excess HFSE accompanying elevated $^{3}He/^{4}He$ (Jackson et al., 2008). For example, within the HSDP-2 dataset there is a negative correlation between $\mu^{182}W$ and $^{208}Pb/^{204}Pb$ ($R^2 = 0.3$; p-value = 0.03) and positive correlation between $^{3}He/^{4}He$ and $^{208}Pb/^{204}Pb$ ($R^2 = 0.6$; p-value < 0.001; Fig. 5C,F). The expression of greater magnitude $\mu^{182}W$ deficits in Mauna Kea could thus be related to elevated abundances of the HFSE Th, as well as time-integrated Th/Pb of the source characterized by negative $\mu^{182}W$, compared to Mauna Kea lavas with normal $\mu^{182}W$. For the Mauna Kea suite there are also statistically significant negative correlations between $\mu^{182}W$ and Ti/Ti* ($Ti/Ti^*=Ti_N/(Sm_N*Tb_N)^{0.5}$), as well as Nb/Nb* ($Nb/Nb^*=Nb_N/(La_N*Th_N)^{0.5}$), linking negative $\mu^{182}W$ anomalies to an excess of the refractory, HFSE Ti and Nb, relative to similarly incompatible elements (Fig. 5A-B). Consistent with the global dataset (Jackson et al., 2008), the correlations between $^{3}He/^{4}He$ and Ti/Ti* and Nb/Nb* are also significant (Fig. 5D-E).

Variations in Ti/Ti* and Nb/Nb* in OIB have been attributed to processes, such as partial melting and/or fractional crystallization and assimilation (Peters and Day, 2014), or may reflect mixing between mantle sources with different Ti and Nb concentrations (Jackson et al., 2008; Prytulak and Elliott, 2007). Assimilation and fractional crystallization (AFC) of oceanic crust during OIB petrogenesis can produce positive Ti/Ti* and Nb/Nb* that positively correlate with whole rock MgO wt.% and olivine and pyroxene modal abundances (Peters and Day, 2014). Within the HSDP-2 dataset, however, Ti/Ti* and Nb/Nb* do not correlate with MgO wt.%, or other major element systematics, such as CaO/Al_2O_3, an indicator of pyroxene fractionation (Supplementary Figure S10). Further, it is unlikely that $\mu^{182}W$ and $^{3}He/^{4}He$ would be equivalently affected by AFC processes to produce the correlations observed in Fig. 5. Elevated Ti/Ti* and Nb/Nb* are also not likely due to an excess of a Ti-rich phase(s) in the Mauna Kea lavas, such as rutile, because Ti/Ti* and Nb/Nb* do not correlate with bulk rock TiO_2 wt.% (Supplementary Figure S10).

The involvement of different phases related to depth of melting could also result in elevated Ti/Ti* and Nb/Nb*. Rare earth element systematics, for example small variations in Gd/Yb, of the HSDP-2 drill core indicate that the older, stratigraphically lower lavas, where the greatest $\mu^{182}W$ deficits and $^{3}He/^{4}He$ are observed, were produced by higher degree partial melts, and that the degree of partial melting tapered off over time as Gd/Yb increased stratigraphically upward (Feigenson et al., 2003). The expression of high $^{3}He/^{4}He$ and negative $\mu^{182}W$, in addition to elevated Ti/Ti* and Nb/Nb*, in the plume may be related to a higher degree of partial melting. The $^{3}He/^{4}He$ of the drill core lavas anti-correlates with Gd/Yb ($R^2 = 0.4$; p-value = 0.007), although $\mu^{182}W$ is not well-correlated with Gd/Yb ($R^2 = 0.2$; p-value = 0.13) within the precision of the current dataset (Supplementary Figure S11). The $\mu^{182}W$ and trace element systematics point to high temperature melting of a less fusible component in the generation of negative $\mu^{182}W$ and high $^{3}He/^{4}He$ in the erupted basalts. Therefore, we conclude elevated Ti/Ti* and Nb/Nb* are primary characteristics of the negative $\mu^{182}W$ mantle source. This conclusion then begs the question of how the elevated Ti/Ti* and Nb/Nb* (and potentially Th) were generated in relation to the anomalous W-He characteristics.

Subchondritic Ti/Zr and Nb/La in the DMM (and continental crust) has been taken as evidence for the existence of a complementary Ti- and Nb-rich reservoir, such as recycled crust in the form of eclogite accumulated in the lower mantle (Jackson et al., 2008; McDonough, 1991). Such material, however, would be unlikely to host low $\mu^{182}W$ and high $^{3}He/^{4}He$, given that most of this material would have accumulated subsequent to the disappearance of ^{182}Hf, and likely experienced He degassing. Thus, if the Ti, Nb, and potentially Th, enrichment in the anomalous component is associated with recycled crust, the correlations must be attributed to a physical juxtaposition of recycled eclogite and lower mantle domain(s) already characterized by anomalous $\mu^{182}W$ and $^{3}He/^{4}He$ (Jackson et al., 2008). Isotopic equilibration between recycled eclogite at the core-mantle boundary and the outer core could potentially produce a reservoir with high Ti/Ti*, Nb/Nb*, and negative $\mu^{182}W$. Diffusion of He from the core could also potentially transfer high

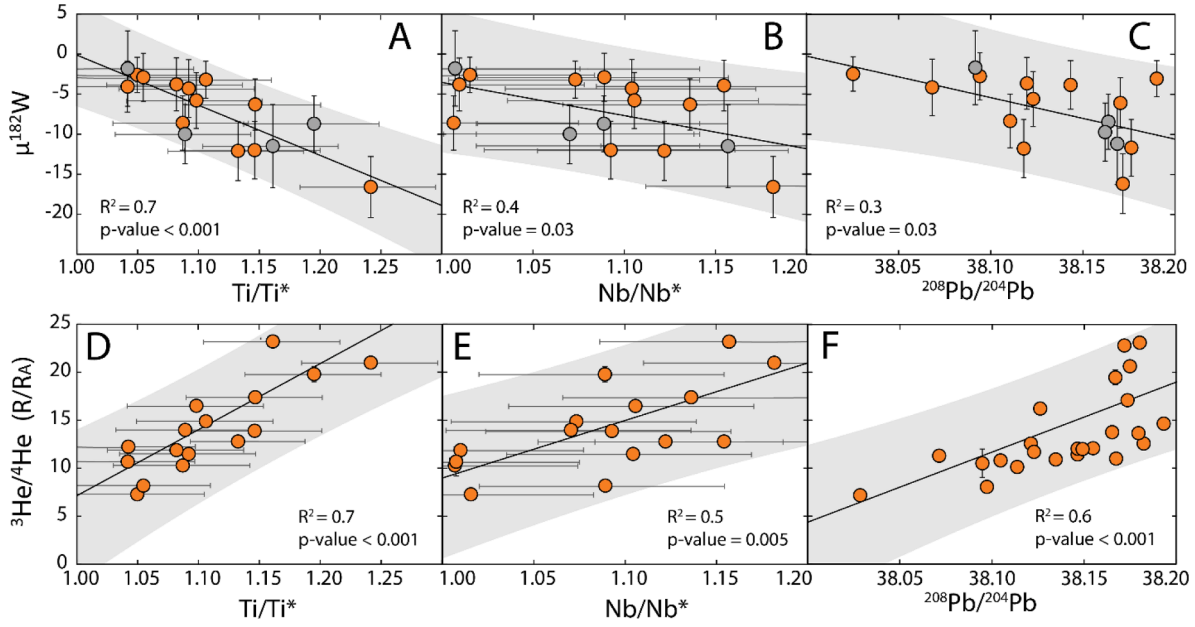

Fig. 5. Tungsten and helium isotopic compositions correlate with Ti/Ti* (A, D), Nb/Nb* (B, E), and $^{208}Pb/^{204}Pb$ (C, F). Error bars represent the 2SE for $\mu^{182}W$ and $^{208}Pb/^{204}Pb$ and 1σ for $^{3}He/^{4}He$. Linear regressions are plotted as black lines with grey bands representing the 95% confidence interval of the regression. Grey circles are previously published $\mu^{182}W$ (Mundl et al., 2017; Mundl-Petermeier et al., 2020). Helium data is from Kurz et al. (2004). Trace element data are from Huang and Frey (2003) and Rhodes and Vollinger (2004). Error bars for Ti/Ti* and Nb/Nb*are calculated by propagating the 1SD of Ti, Nb, Sm, Tb, La, and Th measurements through each ratio.

$^{3}He/^{4}He$ to the recycled eclogitic component at the core-mantle boundary, as the recycled material itself would be unlikely to host high $^{3}He/^{4}He$ (Hanyu and Kaneoka, 1997; Moreira et al., 2003; Moreira and Kurz, 2001). Nevertheless, there is considerable debate with regard to the He content of the core as well as its isotopic composition (Bouhifd et al., 2013; Horton et al., 2023; Ozgurel and Caracas, 2023; Roth et al., 2019). Although the core formed early in Earth history, its $^{3}He/^{4}He$ may not be as high as in primitive materials, given that its composition through time would be dependent on the concentration of He relative to that of the ^{4}He producing elements, U, Th, and Pt present in the core (Ozgurel and Caracas, 2023). Furthermore, a high Re/Os eclogitic component in the mantle source would be expected to produce radiogenic $^{187}Os/^{188}Os$, which is in contrast to the relatively un-radiogenic $^{187}Os/^{188}Os$ of Mauna Kea compared to other Hawaiian volcanic centers; therefore, this is considered an unlikely model.

Another mechanism that could lead to elevated Ti/Ti* and Nb/Nb* in mantle-derived rocks is melt equilibration with a bridgmanite and Ca-perovskite bearing lithology in the lower mantle, due to the relatively low partition coefficients of Ti and Nb in perovskites compared to rare earth elements and U (Hirose et al., 2004; Jackson et al., 2008). A basal magma ocean with high Ti/Ti* and Nb/Nb* could experience isotopic equilibration with the core at any point in Earth's history to acquire negative $\mu^{182}W$ (Mundl-Petermeier et al., 2020). Alternatively, an early magma ocean that equilibrated with bridgmanite and Ca-perovskite while ^{182}Hf was extant may also be characterized by a low Hf/W, due to the preferential compatibility of Hf, relative to W, in the two perovskite phases (Brown et al., 2014; Corgne et al., 2005), and would therefore evolve to a lower $\mu^{182}W$ than the crystallizing solid. In this case, a single process might have generated high Ti/Ti* and Nb/Nb* and negative $\mu^{182}W$. The envisioned deep, primitive reservoir, however, must have retained isotopic signatures that pre-date the Moon-forming giant impact event. This early-formed reservoir might also have developed a low Sm/Nd, and therefore, evolve negative $\mu^{142}Nd$ (Brown et al., 2014). Limited available data do not show a correlation between $\mu^{182}W$ and $\mu^{142}Nd$ in Hawaii (Horan et al., 2018). It is also possible that the degree of fractionation between Sm and Nd was insufficient to generate discernable $\mu^{142}Nd$ variability, as the partition coefficients for Sm and Nd in perovskite may be more similar compared to Hf and W (Brown et al., 2014). Additionally, recycling of lithospheric material with a high Nd/W would preferentially erase $\mu^{142}Nd$ variability compared to $\mu^{182}W$. This may be likely due to the high Nd/W in mantle-derived rocks (Arevalo and McDonough, 2010) and bulk continental crust (Rudnick and Gao, 2003), as well as the fluid mobility of W during subduction that may remove W from the down-going slab (Bali et al., 2012). Therefore, if $\mu^{182}W$ and $\mu^{142}Nd$ were correlated in an early, deep mantle magma ocean, $\mu^{142}Nd$ variability may have since been overprinted.

We conclude that either diffusional equilibration of W, and possibly He, between the core and a HFSE-enriched portion of the mantle occurring at the core-mantle boundary, or very early crystal-liquid fractionation associated with magma ocean crystallization occurring in the deep mantle, can potentially account for the origin of the isotopically anomalous component identified in the Mauna Kea suite. Geophysical evidence supports the presence of a km-scale physically distinct layer, such as a remnant magma ocean or iron-enriched domain possibly related to ultra-low velocity zones, at the core-mantle boundary, where long-term storage of He and ancient geochemical signatures (e.g., low $\mu^{182}W$ and high $^{3}He/^{4}He$) and/or core-mantle interaction is also plausible (Labrosse et al., 2007; Russell et al., 2023; Williams and Garnero, 1996). Uncertainties in the concentration and isotopic composition of He in the core or an early magma ocean, diffusion characteristics of W and He at the CMB, and partitioning behaviors of Hf and W at high pressures and temperatures preclude a more definitive determination of the origin of the anomalous component.

4.4. Implications for plume structure and dynamics

The stratigraphic series of $\mu^{182}W$ presented here provides an opportunity to investigate plume structure and dynamics from a W isotopic perspective. Pre-existing plume models for Hawaii include a concentrically zoned plume in which primitive material containing high $^{3}He/^{4}He$ is located at the axis of the plume where the temperature is highest (Bryce et al., 2005; DePaolo et al., 2001). A contrasting model for the Hawaiian plume is a bilaterally zoned plume that produces the geographic and chemical Kea and Loa trend volcanic chains (Abouchami et al., 2005). A third model, which is not mutually exclusive from either a concentrically or bilaterally zoned plume, includes vertical heterogeneity with "blobs" or elongated "filaments" of anomalous material (e.g., recycled or primitive material) that can cause isotopic variations over time and space in Hawaiian volcanics (Blichert-Toft et al., 2003; Bryce et al., 2005; Eisele et al., 2003; Farnetani and Hofmann, 2009).

To test whether the $\mu^{182}W$ systematics of HSDP-2 can be explained by any of these plume models, we examine the stratigraphic data as a function of time and location of the Mauna Kea and Mauna Loa volcanoes relative to the inferred plume center. First, we consider a concentrically zoned plume to calculate the expected isotopic composition of the HSDP-2 core as Mauna Kea (and Mauna Loa) recede from the plume axis. In this model, the isotopic composition of the plume center is defined by the highest $^{3}He/^{4}He$ (32.2 R/R_A) and greatest magnitude $\mu^{182}W$ deficit (−25.6) measured in Hawaiian lavas (Kent et al., 1999; Mundl-Petermeier et al., 2020). The most distal portion of the plume is defined by "normal" mantle $^{3}He/^{4}He$ (~8 R/R_A) (Graham, 2002) and $\mu^{182}W$ (~0) (Kleine and Walker, 2017). To model the isotopic composition of the HSDP-2 drill core that would result from a concentrically zoned plume, we calculate the isotopic ratio of a given element (i.e., He, Sr, Hf, W, Os, Pb) as a function of radial distance from the plume axis. The axis is assigned the maximum (or minimum) value for each isotopic ratio of interest and the ratio changes exponentially with radial distance according to $R = R_{min} + (R_{max} - R_{min}) \times e^{\frac{r^2}{a^2}}$, and expresses the isotopic ratio, R, of a given element as a function of radial distance, r, from the plume axis (Bryce et al., 2005). There is also a parameter for the length-scale of isotopic heterogeneity, a, that controls how rapidly the ratio changes with radius, r (Bryce et al., 2005). Further details on the calculation can be found in the supplementary material.

We find that a concentrically zoned plume with anomalous $^{3}He/^{4}He$ and $\mu^{182}W$ could produce the greatest magnitude anomalies and temporal decrease in the magnitude of $\mu^{182}W$ and $^{3}He/^{4}He$ in Mauna Kea (Fig. 6). The reappearance of $\mu^{182}W$ deficits and elevated $^{3}He/^{4}He$ in the Mauna Loa volcanics may be due to the relative proximity of Mauna Loa to the plume axis at ~200 ka compared to the Mauna Kea volcano sampled just prior in the stratigraphic column. The presence of "normal" $\mu^{182}W$ and moderate deficits throughout the entire Mauna Kea stratigraphic sequence requires that ambient mantle-like $^{3}He/^{4}He$ and $\mu^{182}W$ coexist in the melt region. Thus, the calculated isotopic compositions in the concentrically zoned plume model reflect only the maximum magnitude $^{3}He/^{4}He$ and $\mu^{182}W$ values (Fig. 6). Compositional zoning, and/or a temperature-dependent process, like relative partial melting of variably fusible components, are plausible as the distance of a volcano from the plume center also scales with a decrease in plume temperature.

A concentrically zoned plume fails to explain the lack of variation observed in $^{87}Sr/^{86}Sr$, $^{176}Hf/^{177}Hf$, $^{206}Pb/^{204}Pb$, $^{207}Pb/^{204}Pb$, and $^{187}Os/^{188}Os$ in the Mauna Kea stratigraphic column, since the ratios should systematically change with radial distance from the plume center (Supplementary Figure S12). Of note, however, is that the model seems to better capture Mauna Loa Hf and Pb isotopic compositions (Supplementary Figure S12). This requires a more complex plume structure than compositional concentric zoning to capture the isotope systematics of both volcanoes.

An alternative structural model for the Hawaiian mantle plume invokes a bilateral or azimuthal zonation that can explain the Loa and Kea

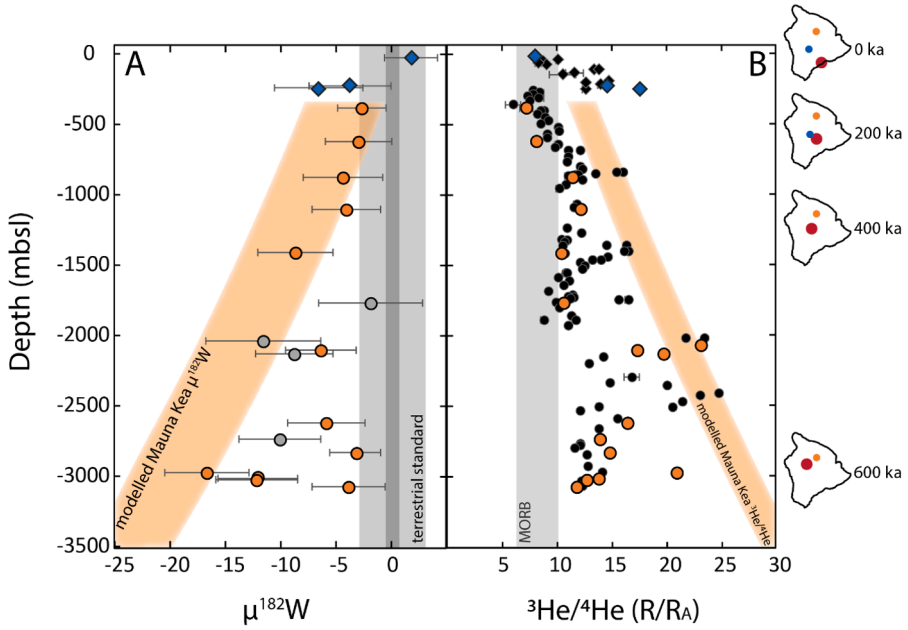

Fig. 6. Tungsten-182 and $^{3}He/^{4}He$ as a function of stratigraphic depth in meters below sea level (mbsl). The orange fields represent the calculated isotopic composition of Mauna Kea in the drill core based on a concentrically zoned plume (see Section 4.4). Far right: The relative location of Mauna Kea (orange circle) and Mauna Loa (blue circle), respectively, from the inferred plume core (red circle) over the ~600,000 year interval captured by HSDP-2. (A) Orange symbols are data from this study and grey symbols are previous $\mu^{182}W$ measurements (Mundl et al., 2017; Mundl-Petermeier et al., 2020). Blue diamonds are new $\mu^{182}W$ measurements for Mauna Loa volcanics from HSDP-2. Vertical grey bands reflect the 2SD (light grey) and 2SE (dark grey) external reproducibility of the Alfa Aesar W standard. (B) Orange and blue symbols represent the samples that have also been characterized for $\mu^{182}W$. Black circles and diamonds represent $^{3}He/^{4}He$ measurements that do not have paired $\mu^{182}W$ analyses. All He data are from Kurz et al. (2004). The vertical grey band reflects the typical range of $^{3}He/^{4}He$ (8 ± 2 R/R_A) observed in global MORB distal from mantle plumes (Graham, 2002).

trends observed across several Hawaiian islands (Abouchami et al., 2005). One interpretation is that the geochemically enriched Loa trend characteristics result from the entrainment of a physically distinct deep mantle component associated with recycled and/or primitive material, and the Kea trend samples the ambient, deep Pacific mantle (Harrison et al., 2017; Weis et al., 2020, 2011). Tungsten isotopic data for three Kea trend volcanoes (Kohala, Mauna Kea, and Kīlauea) and two Loa trend volcanoes (Mauna Loa and Kama'ehuakanaloa) show that both trends produce rocks with negative $\mu^{182}W$ (Archer et al., 2023; Mundl et al., 2017; Mundl-Petermeier et al., 2020). Despite distinct componentry defining the lithophile isotopic compositions of the Kea and Loa trends, within HSDP-2, Mauna Loa samples have a $^{3}He/^{4}He$ versus $\mu^{182}W$ slope that is indistinguishable from Mauna Kea, indicating there is no bilateral difference in the W-He systematics of the Hawaiian plume. It is concluded that the component(s) hosting $\mu^{182}W$ deficits and high $^{3}He/^{4}He$ are sampled by both Loa and Kea trends and are thus independent of any bilateral zonation intrinsic to the plume. It remains likely, however, that the Loa trend samples a distinct deep component(s) with respect to radiogenic lithophile isotopic systems (Harrison et al., 2017; Weis et al., 2020, 2011). Strategic sampling from both younger and older Loa and Kea trend volcanoes will be necessary to identify differences, if any, in W-He systematics between the two trends.

Vertical heterogeneity in the plume may also explain the temporal trends observed in HSDP-2. A vertical "pulse" or "blob" of anomalous material may produce high $^{3}He/^{4}He$ and $\mu^{182}W$ deficits in volcanic products for a period of time that correlates with the size of the "pulse" (Farnetani et al., 2018; Farnetani and Hofmann, 2010, 2009). It is possible that $\mu^{182}W$ deficits exist at equal or greater magnitude in the Mauna Kea volcanics below the HSDP-2 drill core stratigraphy, making it impossible to constrain the size of a hypothetical, anomalous "filament" or "blob" in the plume source. Of the characterized lavas, the first resolvable $\mu^{182}W$ deficit appears at ~620 ka and the last resolvable $\mu^{182}W$ deficit occurs at ~440 ka, giving a minimum ~180 kyr duration of sampling anomalous material at Mauna Kea. Assuming the vertical velocity of the plume is a maximum of 34 cm/yr at the axis and decreases exponentially to 2 cm/yr at the edge (Watson and McKenzie, 1991), integration across the ~180 kyr Mauna Kea record where resolvable $\mu^{182}W$ deficits are present may constrain the minimum vertical height of the isotopically anomalous portion of the solid plume that was sampled during that interval. The minimum approximate vertical height required to produce ~180 kyr of anomalous $\mu^{182}W$ is ~30 km (see Supplementary Material S.6 for calculation). A vertically heterogenous model would further require a coincidence to produce the systematic appearance and dissipation of $^{3}He/^{4}He$ and $\mu^{182}W$ anomalies in HSDP-2 in both Mauna Kea and Mauna Loa as they move away from the plume axis. A second "blob" is then required to reintroduce anomalous $\mu^{182}W$ at the beginning of the Mauna Loa stratigraphic section in HSDP-2. Therefore, although plausible, a "pulsing" plume appears unlikely to explain HSDP-2 $\mu^{182}W$ stratigraphy. It is more likely that vertical heterogeneity coexists within a concentrically and/or azimuthally zoned plume in the form of elongated filaments that span beyond the timescale of the HSDP-2 drill core (Farnetani et al., 2018; Farnetani and Hofmann, 2010, 2009).

5. Conclusions

Mauna Kea volcanics are characterized by $\mu^{182}W$ values ranging from those similar to the modern BSE to negative $\mu^{182}W$ values that are well-resolved from the terrestrial standard. Generally, $\mu^{182}W$ is correlated with $^{3}He/^{4}He$ in Mauna Kea and the W-He systematics can be explained by two-component mixing. The elevated Ti/Ti* and Nb/Nb* observed in lavas with $\mu^{182}W$ deficits indicates that a refractory component likely hosts the negative $\mu^{182}W$ and high $^{3}He/^{4}He$. This component may have originated solely as a result of early Earth crystal-liquid fractionation processes in the deep mantle, or as a result of diffusional equilibration of W and possibly He between the core and the mantle coupled with an early magma ocean fractionation product at the core-mantle boundary. The HSDP-2 stratigraphy shows that $\mu^{182}W$ deficits and $^{3}He/^{4}He$ are

greatest when the Mauna Kea volcano was nearest the plume axis. The refractory component hosting negative $\mu^{182}W$ and high $^{3}He/^{4}He$ may be more easily melted at the plume axis where the temperature is highest compared to cooler, distal regions of the plume. The two defining type locality volcanoes for the Kea and Loa trends, Mauna Kea and Mauna Loa, respectively, do not show distinct $\mu^{182}W$ and $^{3}He/^{4}He$ systematics with the available data. This observation indicates that anomalous $\mu^{182}W$ is likely independent of the distinct mantle components that produce the Loa and Kea trend geochemical characteristics in Hawaii.

CRediT authorship contribution statement

Lori N Willhite: Conceptualization, Methodology, Investigation, Formal analysis, Data curation, Visualization, Writing – original draft, Writing – review & editing. **Valerie A Finlayson:** Conceptualization, Methodology, Investigation, Writing – review & editing, Funding acquisition. **Richard J Walker:** Conceptualization, Supervision, Investigation, Resources, Writing – review & editing, Funding acquisition.

Declaration of competing interest

The authors declare that they have no known competing financial interests or personal relationships that could have appeared to influence the work reported in this paper.

Data availability

Data will be made available on request.

Acknowledgements

This work was supported by NSF-EAR #2121979 to R. J. W. and V. A. F. The authors would like to thank Saebyul Choe for her assistance with drill core sampling and curation at the American Museum of Natural History, and Andrew Houston for his assistance with sample preparation at UMD. We thank Hanika Rizo and an anonymous reviewer for their comments that improved this manuscript. The authors thank Fang-Zhen Teng for the editorial handling of this manuscript.

Supplementary materials

Supplementary material associated with this article can be found, in the online version, at doi:10.1016/j.epsl.2024.118795.

References

Abouchami, W., Hofmann, A.W., Galer, S.J.G., Frey, F.A., Eisele, J., Feigenson, M., 2005. Lead isotopes reveal bilateral asymmetry and vertical continuity in the Hawaiian mantle plume. Nature 434, 851–856. https://doi.org/10.1038/nature03402.

Archer, G.J., Budde, G., Worsham, E.A., Stracke, A., Jackson, M.G., Kleine, T., 2023. Origin of ^{182}W anomalies in ocean island basalts. Geochem., Geophys., Geosyst. 24 https://doi.org/10.1029/2022GC010688 e2022GC010688.

Archer, G.J., Mundl, A., Walker, R.J., Worsham, E.A., Bermingham, K.R., 2017. High-precision analysis of $^{182}W/^{184}W$ and $^{183}W/^{184}W$ by negative thermal ionization mass spectrometry: per-integration oxide corrections using measured $^{18}O/^{16}O$. Int. J. Mass Spectrom. 414, 80–86. https://doi.org/10.1016/j.ijms.2017.01.002.

Arevalo, R., McDonough, W.F., 2010. Chemical variations and regional diversity observed in MORB. Chem. Geol. 271, 70–85. https://doi.org/10.1016/j.chemgeo.2009.12.013.

Arevalo, R., McDonough, W.F., 2008. Tungsten geochemistry and implications for understanding the Earth's interior. Earth Planet. Sci. Lett. 272, 656–665. https://doi.org/10.1016/j.epsl.2008.05.031.

Bali, E., Keppler, H., Audetat, A., 2012. The mobility of W and Mo in subduction zone fluids and the Mo–W–Th–U systematics of island arc magmas. Earth Planet. Sci. Lett. 351–352, 195–207. https://doi.org/10.1016/j.epsl.2012.07.032.

Ballentine, C.J., van Keken, P.E., Porcelli, D., Hauri, E.H., 2002. Numerical models, geochemistry and the zero–paradox noble–gas mantle. Philos. Trans. R. Soc. Lond. Ser. A 360, 2611–2631. https://doi.org/10.1098/rsta.2002.1083.

Becker, H., Horan, M.F., Walker, R.J., Gao, S., Lorand, J.-P., Rudnick, R.L., 2006. Highly siderophile element composition of the Earth's primitive upper mantle: constraints from new data on peridotite massifs and xenoliths. Geochim. Cosmochim. Acta 70, 4528–4550. https://doi.org/10.1016/j.gca.2006.06.004.

Blichert-Toft, J., Weis, D., Maerschalk, C., Agranier, A., Albarède, F., 2003. Hawaiian hot spot dynamics as inferred from the Hf and Pb isotope evolution of Mauna Kea volcano. Geochem., Geophys., Geosyst. 4 https://doi.org/10.1029/2002GC000340.

Bouhifd, M.A., Jephcoat, A.P., Heber, V.S., Kelley, S.P., 2013. Helium in Earth's early core. Nat. Geosci. 6, 982–986. https://doi.org/10.1038/ngeo1959.

Brandon, A.D., Norman, M.D., Walker, R.J., Morgan, J.W., 1999. ^{186}Os–^{187}Os systematics of Hawaiian picrites. Earth Planet. Sci. Lett. 174, 25–42. https://doi.org/10.1016/S0012-821X(99)00251-4.

Brown, S.M., Elkins-Tanton, L.T., Walker, R.J., 2014. Effects of magma ocean crystallization and overturn on the development of ^{142}Nd and ^{182}W isotopic heterogeneities in the primordial mantle. Earth Planet. Sci. Lett. 408, 319–330. https://doi.org/10.1016/j.epsl.2014.10.025.

Bryce, J., Depaolo, D., Lassiter, J., 2005. Geochemical structure of the Hawaiian plume: sr, Nd, and Os isotopes in the 2.8 km HSDP-2 section of Mauna Kea Volcano. Geochem. Geophys. Geosyst. 6 (2005), 6. https://doi.org/10.1029/2004GC000809.

Corgne, A., Liebske, C., Wood, B.J., Rubie, D.C., Frost, D.J., 2005. Silicate perovskite-melt partitioning of trace elements and geochemical signature of a deep perovskitic reservoir. Geochim. Cosmochim. Acta 69, 485–496. https://doi.org/10.1016/j.gca.2004.06.041.

DePaolo, D.J., Bryce, J.G., Dodson, A., Shuster, D.L., Kennedy, B.M., 2001. Isotopic evolution of Mauna Loa and the chemical structure of the Hawaiian plume. Geochem., Geophys., Geosyst. 2 https://doi.org/10.1029/2000GC000139.

Eisele, J., Abouchami, W., Galer, S.J.G., Hofmann, A.W., 2003. The 320 kyr Pb isotope evolution of Mauna Kea lavas recorded in the HSDP-2 drill core. Geochem., Geophys., Geosyst. 4 https://doi.org/10.1029/2002GC000339.

Farnetani, C.G., Hofmann, A.W., 2010. Dynamics and internal structure of the Hawaiian plume. Earth Planet. Sci. Lett. 295, 231–240. https://doi.org/10.1016/j.epsl.2010.04.005.

Farnetani, C.G., Hofmann, A.W., 2009. Dynamics and internal structure of a lower mantle plume conduit. Earth Planet. Sci. Lett. 282, 314–322. https://doi.org/10.1016/j.epsl.2009.03.035.

Farnetani, C.G., Hofmann, A.W., Duvernay, T., Limare, A., 2018. Dynamics of rheological heterogeneities in mantle plumes. Earth Planet. Sci. Lett. 499, 74–82. https://doi.org/10.1016/j.epsl.2018.07.022.

Feigenson, M.D., Bolge, L.L., Carr, M.J., Herzberg, C.T., 2003. REE inverse modeling of HSDP2 basalts: evidence for multiple sources in the Hawaiian plume. Geochem., Geophys., Geosyst. 4 https://doi.org/10.1029/2001GC000271.

Ferrick, A.L., Korenaga, J., 2023. Long-term core–mantle interaction explains W-He isotope heterogeneities. Proc. Natl. Acad. Sci. 120 https://doi.org/10.1073/pnas.2215903120 e2215903120.

Gonnermann, H.M., Mukhopadhyay, S., 2007. Non-equilibrium degassing and a primordial source for helium in ocean-island volcanism. Nature 449, 1037–1040. https://doi.org/10.1038/nature06240.

Graham, D.W., 2002. Noble gas isotope geochemistry of mid-ocean ridge and ocean island basalts: characterization of mantle source reservoirs. Rev. Mineral. Geochem. 47, 247–317. https://doi.org/10.2138/rmg.2002.47.8.

Hanyu, T., Kaneoka, I., 1997. The uniform and low $^{3}He/^{4}He$ ratios of HIMU basalts as evidence for their origin as recycled materials. Nature 390, 273–276. https://doi.org/10.1038/36835.

Harrison, L.N., Weis, D., Garcia, M.O., 2017. The link between Hawaiian mantle plume composition, magmatic flux, and deep mantle geodynamics. Earth Planet. Sci. Lett. 463, 298–309. https://doi.org/10.1016/j.epsl.2017.01.027.

Hirose, K., Shimizu, N., van Westrenen, W., Fei, Y., 2004. Trace element partitioning in Earth's lower mantle and implications for geochemical consequences of partial melting at the core–mantle boundary. Phys. Earth Planetary Interiors, Plumes Superplumes 146, 249–260. https://doi.org/10.1016/j.pepi.2002.11.001.

Horan, M.F., Carlson, R.W., Walker, R.J., Jackson, M., Garçon, M., Norman, M., 2018. Tracking Hadean processes in modern basalts with 142-Neodymium. Earth Planet. Sci. Lett. 484, 184–191. https://doi.org/10.1016/j.epsl.2017.12.017.

Horan, M.F., Walker, R.J., Morgan, J.W., Grossman, J.N., Rubin, A.E., 2003. Highly siderophile elements in chondrites. Chemical geology, highly siderophile elements in the earth and meteorites: a volume in honor of john Morgan 196, 27–42. https://doi.org/10.1016/S0009-2541(02)00405-9.

Horton, F., Asimow, P.D., Farley, K.A., Curtice, J., Kurz, M.D., Blusztajn, J., Biasi, J.A., Boyes, X.M., 2023. Highest terrestrial $^{3}He/^{4}He$ credibly from the core. Nature 623, 90–94. https://doi.org/10.1038/s41586-023-06590-8.

Huang, S., Frey, F.A., 2003. Trace element abundances of Mauna Kea basalt from phase 2 of the Hawaii Scientific Drilling Project: petrogenetic implications of correlations with major element content and isotopic ratios. Geochem., Geophys., Geosyst. 4 https://doi.org/10.1029/2002GC000322.

Ireland, T.J., Arevalo, R., Walker, R.J., McDonough, W.F., 2009a. Tungsten in Hawaiian picrites: a compositional model for the sources of Hawaiian lavas. Geochim. Cosmochim. Acta 73, 4517–4530. https://doi.org/10.1016/j.gca.2009.04.016.

Ireland, T.J., Walker, R.J., Garcia, M.O., 2009b. Highly siderophile element and ^{187}Os isotope systematics of Hawaiian picrites: implications for parental melt composition and source heterogeneity. Chem. Geol. 260, 112–128. https://doi.org/10.1016/j.chemgeo.2008.12.009.

Jackson, M.G., Blichert-Toft, J., Halldórsson, S.A., Mundl-Petermeier, A., Bizimis, M., Kurz, M.D., Price, A.A., Harðardóttir, S., Willhite, L.N., Breddam, K., Becker, T.W., Fischer, R.A., 2020. Ancient helium and tungsten isotopic signatures preserved in mantle domains least modified by crustal recycling. Proc. Natl. Acad. Sci. USA 117, 30993–31001. https://doi.org/10.1073/pnas.2009663117.

Jackson, M.G., Hart, S.R., Saal, A.E., Shimizu, N., Kurz, M.D., Blusztajn, J.S., Skovgaard, A.C., 2008. Globally elevated titanium, tantalum, and niobium (TITAN)

in ocean island basalts with high $^{3}He/^{4}He$. Geochem., Geophys., Geosyst. 9 https://doi.org/10.1029/2007GC001876.
Kent, A.J.R., Clague, D.A., Honda, M., Stolper, E.M., Hutcheon, I.D., Norman, M.D., 1999. Widespread assimilation of a seawater-derived component at Loihi Seamount, Hawaii. Geochim. Cosmochim. Acta 63, 2749–2761. https://doi.org/10.1016/S0016-7037(99)00215-X.
Kleine, T., Mezger, K., Münker, C., Palme, H., Bischoff, A., 2004. ^{182}Hf-^{182}W isotope systematics of chondrites, eucrites, and martian meteorites: chronology of core formation and early mantle differentiation in Vesta and Mars. Geochim. Cosmochim. Acta 68, 2935–2946. https://doi.org/10.1016/j.gca.2004.01.009.
Kleine, T., Walker, R.J., 2017. Tungsten isotopes in planets. Annu. Rev. Earth Planet Sci. 45, 389–417. https://doi.org/10.1146/annurev-earth-063016-020037.
Kurz, M.D., Curtice, J., Lott III, D.E., Solow, A., 2004. Rapid helium isotopic variability in Mauna Kea shield lavas from the Hawaiian scientific drilling project. Geochem., Geophys., Geosyst. 5 https://doi.org/10.1029/2002GC000439.
Labrosse, S., Hernlund, J.W., Coltice, N., 2007. A crystallizing dense magma ocean at the base of the Earth's mantle. Nature 450, 866–869. https://doi.org/10.1038/nature06355.
Lassiter, J.C., Hauri, E.H., 1998. Osmium-isotope variations in Hawaiian lavas: evidence for recycled oceanic lithosphere in the Hawaiian plume. Earth Planet. Sci. Lett. 164, 483–496. https://doi.org/10.1016/S0012-821X(98)00240-4.
Mahaffy, P.R., Donahue, T.M., Atreya, S.K., Owen, T.C., Niemann, H.B., 1998. Galileo probe measurements of D/H and $^{3}He/^{4}He$ in Jupiter's atmosphere. Space Sci. Rev. 84, 251–263. https://doi.org/10.1023/A:1005091806594.
McDonough, W.F., 2003. 2.15 - Compositional model for the earth's core. In: Holland, H. D., Turekian, K.K. (Eds.), Treatise On Geochemistry. Pergamon, Oxford, pp. 547–568. https://doi.org/10.1016/B0-08-043751-6/02015-6.
McDonough, W.F., 1991. Partial melting of subducted oceanic crust and isolation of its residual eclogitic lithology. Philos. Trans. 335, 407–418.
Moreira, M., Blusztajn, J., Curtice, J., Hart, S., Dick, H., Kurz, M.D., 2003. He and Ne isotopes in oceanic crust: implications for noble gas recycling in the mantle. Earth Planet. Sci. Lett. 216, 635–643. https://doi.org/10.1016/S0012-821X(03)00554-5.
Moreira, M., Kurz, M.D., 2001. Subducted oceanic lithosphere and the origin of the 'high μ' basalt helium isotopic signature. Earth Planet. Sci. Lett. 189, 49–57. https://doi.org/10.1016/S0012-821X(01)00340-5.
Mundl, A., Touboul, M., Jackson, M.G., Day, J.M.D., Kurz, M.D., Lekic, V., Helz, R.T., Walker, R.J., 2017. Tungsten-182 heterogeneity in modern ocean island basalts. Science (1979) 356, 66–69. https://doi.org/10.1126/science.aal4179.
Mundl-Petermeier, A., Walker, R.J., Fischer, R.A., Lekic, V., Jackson, M.G., Kurz, M.D., 2020. Anomalous ^{182}W in high $^{3}He/^{4}He$ ocean island basalts: fingerprints of Earth's core? Geochim. Cosmochim. Acta 271, 194–211. https://doi.org/10.1016/j.gca.2019.12.020.
Ozgurel, O., Caracas, R., 2023. The magma ocean was a huge helium reservoir in the early Earth. Geochem. Persp. Let. 25, 46–50. https://doi.org/10.7185/geochemlet.2314.
Peters, B.J., Day, J.M.D., 2014. Assessment of relative Ti, Ta, and Nb (TITAN) enrichments in ocean island basalts. Geochem., Geophys., Geosyst. 15, 4424–4444. https://doi.org/10.1002/2014GC005506.
Peters, B.J., Mundl-Petermeier, A., Finlayson, V.A., 2023. A multi-siderophile element connection between volcanic hotspots and Earth's core. Earth Planetary Sci. Lett. 618, 118285 https://doi.org/10.1016/j.epsl.2023.118285.
Peters, D., Rizo, H., O'Neil, J., Hamelin, C., Shirey, S.B., 2024. Comparative ^{142}Nd and ^{182}W study of MORBs and the 4.5 Gyr evolution of the upper mantle. Geochem. Perspect. Lett. 29, 51–56. https://doi.org/10.7185/geochemlet.2412.
Pitcher, L., Helz, R.T., Walker, R.J., Piccoli, P., 2009. Fractionation of the platinum-group elments and Re during crystallization of basalt in Kilauea Iki Lava Lake, Hawaii. Chem. Geol. 260, 196–210. https://doi.org/10.1016/j.chemgeo.2008.12.022.
Prytulak, J., Elliott, T., 2007. TiO2 enrichment in ocean island basalts. Earth Planet. Sci. Lett. 263, 388–403. https://doi.org/10.1016/j.epsl.2007.09.015.
Puchtel, I.S., Blichert-Toft, J., Touboul, M., Horan, M.F., Walker, R.J., 2016. The coupled ^{182}W-^{142}Nd record of early terrestrial mantle differentiation. Geochem., Geophys., Geosyst. 17, 2168–2193. https://doi.org/10.1002/2016GC006324.
Rhodes, J.M., Vollinger, M.J., 2004. Composition of basaltic lavas sampled by phase-2 of the Hawaii Scientific Drilling Project: geochemical stratigraphy and magma types. Geochem., Geophys., Geosyst. 5 https://doi.org/10.1029/2002GC000434.
Rizo, H., Andrault, D., Bennett, N.R., Humayun, M., Brandon, A., Vlastelic, I., Moine, B., Poirier, A., Bouhifd, M.A., Murphy, D.T., 2019. ^{182}W evidence for core-mantle interaction in the source of mantle plumes. Geochem. Persp. Let. 6–11. https://doi.org/10.7185/geochemlet.1917.
Roth, A.S.G., Liebske, C., Maden, C., Burton, K.W., Schönbächler, M., Busemann, H., 2019. The primordial He budget of the Earth set by percolative core formation in planetesimals. Geochem. Persp. Let. 26–31. https://doi.org/10.7185/geochemlet.1901.
Rudnick, R.L., Gao, S., 2003. 3.01 - Composition of the continental crust. In: Holland, H. D., Turekian, K.K. (Eds.), Treatise On Geochemistry. Pergamon, Oxford, pp. 1–64. https://doi.org/10.1016/B0-08-043751-6/03016-4.
Russell, S., Irving, J.C.E., Jagt, L., Cottaar, S., 2023. Evidence for a kilometer-scale seismically slow layer atop the core-mantle boundary from normal modes. Geophys. Res. Lett. 50 https://doi.org/10.1029/2023GL105684 e2023GL105684.
Sharp, W.D., Renne, P.R., 2005. The $^{40}Ar/^{39}Ar$ dating of core recovered by the Hawaii Scientific Drilling Project (phase 2), Hilo, Hawaii. Geochem., Geophys., Geosyst. 6 https://doi.org/10.1029/2004GC000846.
Touboul, M., Puchtel, I.S., Walker, R.J., 2012. ^{182}W evidence for long-term preservation of early mantle differentiation products. Science. https://doi.org/10.1126/science.1216351.
Vockenhuber, C., Oberli, F., Bichler, M., Ahmad, I., Quitté, G., Meier, M., Halliday, A.N., Lee, D.-C., Kutschera, W., Steier, P., Gehrke, R.J., Helmer, R.G., 2004. New half-life measurement of ^{182}Hf: improved chronometer for the early Solar System. Phys. Rev. Lett. 93, 172501 https://doi.org/10.1103/PhysRevLett.93.172501.
Walker, R.J., Mundl-Petermeier, A., Puchtel, I.S., Nicklas, R.W., Hellmann, J.L., Echeverría, L.M., Ludwig, K.D., Bermingham, K.R., Gazel, E., Devitre, C.L., Jackson, M.G., Chauvel, C., 2023. ^{182}W and ^{187}Os constraints on the origin of siderophile isotopic heterogeneity in the mantle. Geochim. Cosmochim. Acta 363, 15–39. https://doi.org/10.1016/j.gca.2023.11.003.
Watson, S., McKenzie, D., 1991. Melt generation by plumes: a study of Hawaiian volcanism. J. Petrol. 32, 501–537. https://doi.org/10.1093/petrology/32.3.501.
Weis, D., Garcia, M.O., Rhodes, J.M., Jellinek, M., Scoates, J.S., 2011. Role of the deep mantle in generating the compositional asymmetry of the Hawaiian mantle plume. Nat. Geosci. 4, 831–838. https://doi.org/10.1038/ngeo1328.
Weis, D., Harrison, L.N., McMillan, R., Williamson, N.M.B., 2020. Fine-scale structure of Earth's deep mantle resolved through statistical analysis of Hawaiian basalt geochemistry. Geochem., Geophys., Geosyst. 21 https://doi.org/10.1029/2020GC009292 e2020GC009292.
Willbold, M., Elliott, T., Moorbath, S., 2011. The tungsten isotopic composition of the Earth's mantle before the terminal bombardment. Nature 477, 195–198. https://doi.org/10.1038/nature10399.
Williams, Q., Garnero, E.J., 1996. Seismic evidence for partial melt at the base of Earth's mantle. Science (1979) 273, 1528–1530. https://doi.org/10.1126/science.273.5281.1528.
Yoshino, T., Makino, Y., Suzuki, T., Hirata, T., 2020. Grain boundary diffusion of W in lower mantle phase with implications for isotopic heterogeneity in oceanic island basalts by core-mantle interactions. Earth Planet. Sci. Lett. 530, 115887 https://doi.org/10.1016/j.epsl.2019.115887.